

Microfluidic Device for Single-Cell Analysis

Aaron R. Wheeler,^{†,‡} William R. Thronset,^{‡,§} Rebecca J. Whelan,[†] Andrew M. Leach,[†] Richard N. Zare,^{*,†} Yish Hann Liao,[§] Kevin Farrell,[§] Ian D. Manger,[§] and Antoine Daridon^{*,§}

Department of Chemistry, Stanford University, Stanford, California 94305-5080, and Fluidigm Corporation, 7100 Shoreline Court, South San Francisco, California 94080

We have developed a novel microfluidic device constructed from poly(dimethylsiloxane) using multilayer soft lithography technology for the analysis of single cells. The microfluidic network enables the passive and gentle separation of a single cell from the bulk cell suspension, and integrated valves and pumps enable the precise delivery of nanoliter volumes of reagents to that cell. Various applications are demonstrated, including cell viability assays, ionophore-mediated intracellular Ca²⁺ flux measurements, and multistep receptor-mediated Ca²⁺ measurements. These assays, and others, are achieved with significant improvements in reagent consumption, analysis time, and temporal resolution over macroscale alternatives.

The ability to perform molecular and cellular analyses of biological systems has grown rapidly over the past two decades.¹ In particular, the advent and refinement of techniques such as DNA sequencing, gene cloning, monoclonal antibody production, cell transfection, amplification methods (such as PCR), and transgenic animal production have fueled this growth. These techniques have spawned an overwhelming number of identified genes, encoded proteins, engineered cell types, and assays for studying these genes, proteins, and cells. As the number of possible combinations of samples, reagents, and assays increases, it has become apparent that novel approaches are necessary to understand and utilize this complexity.¹

One approach to overcoming these difficulties has been to reduce the scale of assays with microfluidics or “lab-on-a-chip” technology.² Microfluidics has been used to perform a variety of biological assays^{3,4} with minimal reagent consumption. In particular, the dimensions (10–100 μm) of microfluidics have made assays of biological cells a popular application.^{5–10} Unfortunately,

cell assays, like other microfluidic methodologies, have suffered from limited means to manipulate fluids and cells. We report a way to overcome these problems and demonstrate a device for single-cell analysis.

Electrokinetic pumping is the most common technique for control of flow in microfluidic devices and has thus been used to manipulate cells.⁵ Unfortunately, the high current and Joule heating that result from using high voltages with typical cell buffers, and the potential for accidental cell lysis in electric fields, make this a nonideal solution. Other creative methods for control of cells in microfluidic devices include carefully controlling hydrostatic pressure heads in device inlets,⁶ using multiple integrated off-chip pumps,^{7,8} and using optical or dielectrophoretic traps.^{9,10} Only the latter offers the capability to isolate and manipulate individual cells; unfortunately, this method is limited to very low (μL/h) solution flow rates and requires sensitive optics, electronics, or both to implement. Clearly, new tools for manipulation in microfluidics are needed for effective implementation of cellular assays.

The recent development of multilayer soft lithography fabrication^{11–18} has greatly improved control of fluids and cells in microfluidic devices. The fundamental advantage of this technique is the capacity to form near-zero dead-volume valves. Valves are formed at the intersection between channels in distinct “control” and “fluidic” layers. As pneumatic pressure is applied to a control channel, the membrane between layers deflects, closing the fluidic channel. The pneumatic system of valves is digitally controlled and, therefore, completely programmable. From the basic building block (valves), more complex control elements (such as peristaltic pumps^{11,12} and rotary mixers¹³) may be constructed. By integrating

* To whom correspondence should be addressed. E-mail: antoine.daridon@fluidigm.com; zare@stanford.edu.

[†] Stanford University.

[‡] Both authors contributed equally to this work.

[§] Fluidigm Corp.

- (1) Maulik, S.; Patel, S. D. *Molecular Biotechnology*; Wiley-Liss, Inc.: New York, 1997.
- (2) Reyes, D. R.; Iossifidis, D.; Auroux, P. A.; Manz, A. *Anal. Chem.* **2002**, *74*, 2623–2636.
- (3) Khandurina, J.; Guttman, A. *J. Chromatogr., A* **2002**, *943*, 159–183.
- (4) Schulte, T. H.; Bardell, R. L.; Weigl, B. H. *Clin. Chim. Acta* **2002**, *321*, 1–10.
- (5) Li, P. C.; Harrison, D. J. *Anal. Chem.* **1997**, *69*, 1564–1568.
- (6) Yang, M.; Li, C. W.; Yang, J. *Anal. Chem.* **2002**, *74*, 3991–4001.
- (7) Kruger, J.; Singh, K.; O'Neill, A.; Jackson, C.; Morrison, A.; O'Brien, P. J. *Micromech. Microeng.* **2002**, *12*, 486–494.

- (8) Schilling, E. A.; Kamholz, A. E.; Yager, P. *Anal. Chem.* **2002**, *74*, 1798–1804.
- (9) Muller, T.; Gradl, G.; Howitz, S.; Shirley, S.; Schnelle, T.; Fuhr, G. *Biosens. Bioelectron.* **1999**, *14*, 247–256.
- (10) Arai, F.; Ichikawa, A.; Ogawa, M.; Fukuda, T.; Horio, K.; Itoigawa, K. *Electrophoresis* **2001**, *22*, 283–288.
- (11) Unger, M. A.; Chou, H. P.; Thorsen, T.; Scherer, A.; Quake, S. R. *Science* **2000**, *288*, 113–116.
- (12) Quake, S. R.; Scherer, A. *Science* **2000**, *290*, 1536–1540.
- (13) Chou, H. P.; Unger, M. A.; Quake, S. R. *Micromed. Microdev.* **2001**, *3*, 323–330.
- (14) Fu, A. Y.; Chou, H. P.; Spence, C.; Arnold, F. H.; Quake, S. R. *Anal. Chem.* **2002**, *74*, 2451–2457.
- (15) Liu, J.; Enzelberger, M.; Quake, S. R. *Electrophoresis* **2002**, *23*, 1531–1536.
- (16) Thorsen, T.; Maerkl, S. J.; Quake, S. R. *Science* **2002**, *298*, 580–584.
- (17) Leach, A. M.; Wheeler, A. R.; Zare, R. N. *Anal. Chem.* **2003**, *75*, 967–972.
- (18) Hansen, C. L.; Skordalakes, E.; Berger, J. M.; Quake, S. R. *Proc. Natl. Acad. Sci. U.S.A.* **2002**, *99*, 16531–16536.

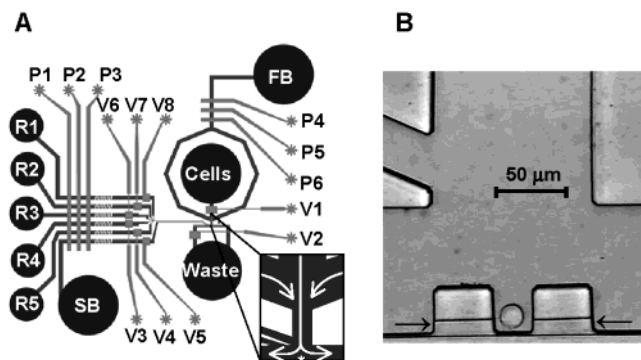


Figure 1. Single-cell analysis device. (A) Schematic of device: fluidic channels are dark; control channels are light. R1–R5 are reactant inlets, SB and FB are shield and focusing buffer inlets, respectively. Valves are actuated by applying pressure to control inlets V1–V8. Pumps are activated by actuating P1–P3 or P4–P6 in series. The serpentine regions of reagent and shield buffer channels diminish flow pulsing resulting from pump activation. Inset: closeup of cell trapping region. Cells are pushed by hydrostatic pressure from cell inlet to waste; they are focused to the center of the stream by the focusing buffer. Note the point of stagnation formed at *. (B) CCD image of an individual Jurkat T-cell trapped in cell dock. Note the drain channels (arrows) on the dock.

many control elements into a single device, a variety of applications has been realized using multilayer soft lithography technology, including, cytometry,¹⁴ PCR,¹⁵ cell microarrays,¹⁶ flow injection analysis,¹⁷ and protein crystallography.¹⁸

We have used this technology to construct a device from poly(dimethylsiloxane) (PDMS) for single-cell assays. In what follows, we describe the operation of this device, present some applications of this device to single-cell analysis, and discuss potential uses.

EXPERIMENTAL SECTION

Fabrication and Characterization of Microfluidic Devices.

The microfluidic devices for cellular analysis (Figure 1) were fabricated from PDMS (RTV 615, GE silicones, Waterford, NY) using multilayer soft lithography fabrication.¹¹ To form the control channels (valves and pumps) and fluidic channels, two positive-relief molds were created using standard photolithographic techniques.

The fluidic mold was formed from three photoresists for fabrication of PDMS channels with three different depths and profiles. Drain channels (Figure 1B) were 10 μm wide and 5 μm deep, with a rectangular profile. Channels that were pumped or valved were 200 μm wide and 20 μm deep, with a semicircular profile. Channels that delivered cells were 100 μm wide and 20 μm deep, with a rectangular profile. The control mold was created using a single photoresist for fabrication of PDMS channels with a depth of 20 μm , with a semicircular profile. Masks for each kind of channel were printed on positive or negative film (depending on photoresist) at 20 000 dpi resolution.

To fabricate the fluidic mold, 5- μm -high features for fabrication of drain channels were prepared first. On a silicon wafer, a layer of SU-8 2005 negative photoresist (MicroChem Corp., Newton, MA) was spin-coated at 3000 rpm and prebaked according to the vendor's instructions. The coated wafer was aligned and exposed (160 mJ/cm^2) through the mask in "direct contact" mode using a

mask aligner (ABM Inc., San Jose, CA). Following exposure, the coated wafer was postbaked and developed by sequential exposure to NANO developer (Microchem), acetone, and 2-propanol (HPLC grade, EMD Chemicals, Gibbstown, NJ). These features (and other SU8 features) had a rectangular profile.

The 20- μm -high features for fabrication of valve (and pump) seats were the second set of features to be patterned onto the fluidic mold. The patterned wafer was placed in a vapor chamber (10 min) in the presence of hexamethyldisilazane (Shin-Etsu Chemical, Tokyo, JP). AZ PLP 100 positive photoresist (Clariant Corp., Sunnyvale, CA) was spin-coated at 2000 rpm and prebaked (100 $^{\circ}\text{C}$, 2 min). A mask was aligned to the SU8 features already patterned on the wafer, and the wafer was exposed (450 mJ/cm^2) through the mask in direct contact mode. Following exposure, the wafer was developed by immersion in AZ 400K (Clariant) developer (1:3 developer/distilled water), rinsed, and dried with N_2 gas. The wafer was then hard baked by ramping up to a temperature of 200 $^{\circ}\text{C}$ (1 $^{\circ}\text{C}/\text{min}$), holding for 1 h, and then ramping down to room temperature (1 $^{\circ}\text{C}/\text{min}$). This procedure caused the PLP-100 photoresist to reflow (for a semicircular profile) and ensured chemical inertness of this layer to the rest of the process. An identical procedure (AZ PLP 100 photoresist only) was used to create the control mold.

The 20- μm -high features for fabrication of cell delivery channels were the final set of features to be patterned onto the fluidic mold. SU-8 2050 negative photoresist was spin-coated at 5000 rpm and prebaked to achieve the desired thickness according to the vendor's instructions. A mask was aligned to the SU8 features already patterned on the coated wafer, and the wafer was exposed (310 mJ/cm^2) through the mask in direct contact mode. Following exposure, the coated wafer was postbaked and developed in the same manner as the first set of 5- μm -high features.

After preparation of the molds, the PDMS device was fabricated using multilayer soft lithography, which has been described elsewhere.^{11,13–15,18} Briefly, the two molds were silanized with trimethylchlorosilane (Puriss grade, Fluka). A thin PDMS layer was spin-coated onto the fluidic mold (~ 90 μm thick), and a thicker PDMS layer was poured onto the control mold (~ 8 mm thick). The layers were cured separately (90 min, 80 $^{\circ}\text{C}$), and the control layer was peeled from the mold, trimmed, and punched to interface with control lines. The control layer was then aligned onto the fluidic layer. The combined layers were cured a second time (90 min, 80 $^{\circ}\text{C}$) to allow chemical bonding. After curing, the chips were peeled from the fluidic mold, trimmed, and punched to create fluid reservoirs. The chip was then bonded to a glass coverslip to seal the fluidic channels.

The chips were used as described previously for similar devices.^{11–18} Pumps and valves were actuated with a digitally controlled manifold of three-way pneumatic switch valves. The manifold controlled compressed nitrogen or helium applied to the device (~ 20 psi); control channels were sometimes filled with water to prevent diffusion of gas bubbles into fluidic channels. Fluidic channels were filled with aqueous buffer with gel-loading pipet tips. Typically, 10–15 μL was pipetted into the large inlets (FB, Cells, Waste, and SB in Figure 1A), and 2–3 μL was pipetted into the small inlets (R1–R5). Solutions were pumped at 5–60 Hz, corresponding to linear flow rates of ~ 300 –1000 $\mu\text{m}/\text{s}$. After repeated use, the chips sometimes became clogged with cellular

debris. Rinsing with 1% sodium dodecyl sulfate or 1 N NaOH restored devices for reuse. A single device was used to analyze up to 20–30 cells. All experiments were performed at room temperature.

When used with cells, the trap worked as described in the Results section. For the larger Jurkat T cells, it was observed that once a single cell was trapped, its presence caused the trap to reject other cells (the trapped cell served as a flow restrictor). For the slightly smaller U937 cells, occasionally more than one cell was trapped. U937 cells were also occasionally observed to flow through the drain channels or remain stuck in the drain channels. Smaller trap geometries could easily solve this problem; in fact, different trap geometries could be developed for a wide distribution of cell dimensions.

Reagents and Cell Culture. Where not otherwise noted, general reagents were from Sigma (St. Louis, MO), cells and culture reagents were from ATCC (Manassas, VA), and fluorescent dyes were from Molecular Probes (Eugene, OR). Jurkat and U937¹⁹ cells were maintained in a humidified atmosphere with 5% CO₂ in growth medium consisting of RPMI 1640 supplemented with 10% fetal bovine serum, penicillin (100 IU/mL), and streptomycin (100 µg/mL). Cells were subcultured twice a week at 1:10 density. Some U937 cells were cultured with IFN-γ (150 ng/mL, 24 h) or dbcAMP (1 mM, 48 h) prior to analysis.

For Jurkat T-cell viability and ionomycin assays, cells were washed and suspended in Hank's balanced saline (HBS, Mediatech, Herndon, VA) supplemented with HEPES (20 mM, pH 7.4). HBS was used for both shield and focusing buffers for on-chip experiments. Trypan blue (0.4 wt %/vol) in HBS was used for the viability assay and to demonstrate load and perfuse states. Prior to calcium flux experiments, Jurkat cells were incubated with Fluo-3/AM ester (5 µM, 30 min, 37 °C). Ionomycin (10 µM) in HBS was used to stimulate calcium flux.

For U937 studies, an S-Ringer saline solution (160 mM NaCl, 5 mM KCl, 2 mM CaCl₂, 1 mM MgCl₂, 5 mM HEPES, pH 7.4) with 0.1 mM sulfapyrazone (to inhibit dye leakage from the cell), was used to wash cells, and as shield/focusing buffer. Prior to calcium flux measurements, U937 cells were incubated with Fluo-4/AM ester (4 µM, 20 min, room temperature). U937 cells often stick to PDMS; thus, chips were typically incubated with bovine serum albumin (BSA) for 20 min (40 mg/mL in S-Ringer) to prevent adhesion. Two stimulants were used to evoke calcium flux, a "primary antibody" (human IgG, 0.75 mg/mL in S-Ringer), and "secondary antibody" (goat anti-human IgG, 5 µM in S-Ringer, with 2 mg/mL BSA). Primary antibody was perfused (pumped at 5 Hz) onto isolated cells for 3 min, followed by perfusion with secondary antibody. Fluorescence was always measured during secondary antibody perfusion, and often during primary antibody, or blank buffer perfusion, to measure "blank" signal.

Experimental System. Epifluorescence experiments were carried out on an inverted microscope (Zeiss, Thornwood, NY) with the 488-nm line of an argon ion laser (Melles Griot, Carlsbad, CA) for excitation. A high NA microscope objective (40× or 100×) was used to focus the laser into the chip. For flow rate measurement, and load/perfuse switching time measurements, a small laser spot (<1 µm) caused food coloring dye in HBS to fluoresce. For excitation of cells, auxiliary optics defocused the laser to a

~50-µm-diameter spot. Laser intensity was attenuated to ~2.5 µW with neutral density filters.

Fluorescence signal was filtered optically (535 ± 25 nm band-pass, 488-nm holographic notch) and spatially (1-mm-diameter pinhole in the back parafocal plane of the microscope) before detection with a photomultiplier tube (PMT). PMT signal was acquired at high frequency into a PC with A/D card and home-written LabView software (National Instruments, Austin, TX).

Signal was displayed as a function of time; high-frequency samples were either averaged into 1-s bins or smoothed by a running average (every 15 points) with Igor Pro software (WaveMetrics, Lake Oswego, OR). For U937 cell calcium flux experiments, a number of parameters, including relative peak heights, duration of signal, and lag time, were extracted from the data. Relative peak heights were defined as the maximum observed signal divided by the average of the preceding baseline (20 s). The duration of the signal was defined as the amount of time that passed between the first point at which the signal rose above 0.1 times the maximum signal and the point (after the maximum) at which the signal decreased below 0.1 times the maximum signal. The lag time was defined as the time that passed between the initiation of perfusion with primary antibody and the point at which the signal rose above 0.1 times the maximum signal.

RESULTS

Microfluidic Chip Design. The microfluidic device used in this study (shown in Figure 1A) has been designed to facilitate two functions: rapid isolation of an individual cell from a mixture of cells in bulk solution and precise delivery of minute volumes of reagents to the selected cell. Our implementation of these functions relies both on the laminar flow characteristics of microfluidic systems and on the ability to manipulate fluids and cells using valves and pumps.

Isolating individual cells from bulk solution is achieved by making use of fluid dynamics at a "T-junction". Under low Reynolds number conditions, when a flowing solution divides into two streams at a T-junction, a point of stagnation²⁰ develops at the center of the T (Figure 1A, inset). By fabricating a "dock" with small drain channels at the point of stagnation, it is possible to stabilize the flow stream such that a cell that lands in the dock becomes trapped (Figure 1B). To increase the efficiency of capture, cells are hydrodynamically focused between two buffer streams. Even when traveling at fairly high flow rates (1 mm/s), cells land gently in the dock and are not subject to significant pressure drops as they would experience in a filter-type trap. Once a cell is trapped, it physically limits the flow through the drain channels and prevents trapping of additional cells.

The reagent delivery function also relies on laminar flow characteristics of microfluidic systems. Two small delivery channels are positioned to the left of the cell dock. The channel nearest to the dock delivers a "shield buffer"; the channel farthest from the dock delivers reagents. By actuating pumps and valves such that the contents of both delivery channels are flowing by the dock, reagents are "loaded" a few micrometers from the cell (Figure 2A, main). If the shield buffer valve is then closed, the reagent(s) can perfuse onto the cell (Figure 2A, inset).

(19) Sundstrom, C.; Nilsson, K. *Int. J. Cancer* **1976**, *17*, 565–577.

(20) Mott, R. L. *Applied Fluid Mechanics*, 5 ed.; Prentice Hall, Inc.: Upper Saddle River, NJ, 2000.

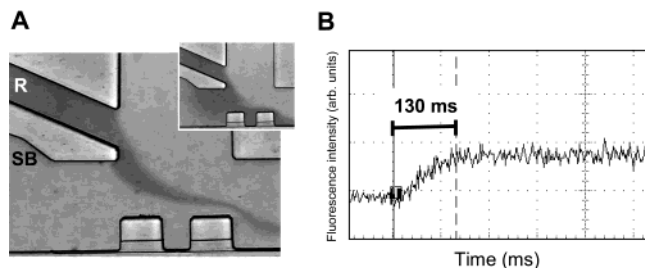


Figure 2. (A) Images of "load" (main) and "perfuse" (inset) states. In the load state, reagents (R) and shield buffer (SB) are both pumped over the dock. In the perfuse state, the shield buffer valve is closed, and the reagents flow onto the dock. (B) Oscilloscope screen capture of dye-marked solution change during a switch from load to perfuse. A complete solution change is achieved in ~ 100 ms.

The reagent delivery system described above forms a perfusion chamber with several advantages over macroscale alternatives. Standard perfusion chambers typically contain $50\text{--}250\ \mu\text{L}$, and complete solution change usually requires ~ 1 s.²¹ In sharp contrast, our "chamber", which is defined by (a) the width and depth of the T-junction ($75 \times 20\ \mu\text{m}$) and (b) 3 times the length of the cell dock ($300\ \mu\text{m}$), corresponds to ~ 0.5 nL. Complete solution change (from "load" to "perfuse" state) can be accomplished in ~ 100 ms (Figure 2B). Thus, for a typical experiment, our device will require $\sim 10^5$ times lower reagent consumption and will allow monitoring of cellular processes that are ~ 10 times faster than standard perfusion chambers.

By alternating appropriate load and perfuse steps with different reagents, we can conduct multistep cell analyses. To demonstrate this capability, a cell viability assay has been conducted. We make sequential perfusion steps of the dye, trypan blue, and methanol, as shown in Figure 3. This dye is known to stain only dead cells. Perfusion conditions are identical for each reagent because all reagents share a common delivery channel (see Figure 1A, R1–R5). Between each perfusion step is a load step; this protects the cell from exposure to mixtures of reagents until a pure flow of the second reagent is established.

The combination of cell isolation and reagent perfusion offers the potential for rapid, low-volume implementations of traditional cellular analyses. To demonstrate this feature, we have performed intracellular calcium ion concentration ($[\text{Ca}^{2+}]_i$) measurements on individual Jurkat T-lymphocytes.

Ionophore-Mediated $[\text{Ca}^{2+}]_i$ Flux. Measurement of $[\text{Ca}^{2+}]_i$ flux is of great interest because of calcium's role as a universal second messenger for cellular processes.²² Calcium flux is usually measured with chemical probes; when loaded into the cytoplasm, the probe reports changes in $[\text{Ca}^{2+}]_i$ with increased or decreased fluorescence. A variety of stimuli have been observed to evoke a wide range of $[\text{Ca}^{2+}]_i$ responses, as determined by the shape, intensity, and temporal dynamics of the measured fluorescence signal.²²

A common calcium flux-evoking stimulus is the membrane-soluble calcium chelator, ionomycin. In T-lymphocytes, low concentrations of ionomycin have been observed to release Ca^{2+}

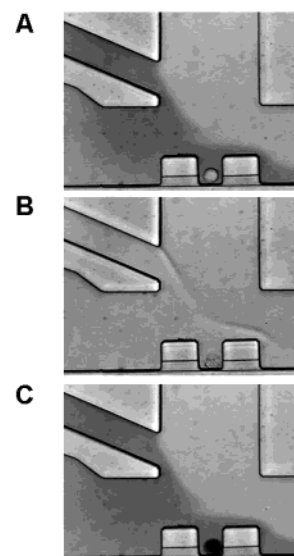


Figure 3. Chronological sequence of images of a viability assay on a single Jurkat T-cell. (A) Live cell perfused with trypan blue dye. Because the cell is healthy, it is not stained. (B) Cell perfused with methanol, which causes permeabilization, followed by cell death. (C) Permeabilized cell perfused with dye; it has rapidly (<5 s) stained. Between each "perfuse" step, reagents are "loaded" (see Figure 2). The entire assay is performed in less than 2 min. A movie of this sequence can be found in Supporting Information.

from internal stores into the cytosol;²³ this release in turn triggers plasmalammellar calcium channels to open, allowing influx from the extracellular media in a process known as store-regulated calcium uptake (SRCU). In single cell studies with T-lymphocytes, ionomycin-stimulated SRCU has been shown to generate $[\text{Ca}^{2+}]_i$ oscillations.²⁴ We have duplicated these experiments using our cell analysis device.

A suspension of Jurkat T-cells (each $\sim 15\ \mu\text{m}$ in diameter) was incubated with Fluo-3 calcium-indicating dye and then loaded into the cell inlet port on the chip. Cells were trapped as described above, and calcium flux was triggered by opening a reagent valve and perfusing with ionomycin. Fluorescent signal was measured and plotted versus time (Figure 4). As reported earlier,^{23,24} individual T-cells often responded with either transient ringing or sustained response, indicative of influx of Ca^{2+} from extracellular buffer.

Unlike standard cell-labeling protocols, in our methodology cells were not "washed" (a time-consuming process of centrifugation and resuspension in dye-free buffer, often performed 2–3 times) prior to analysis. The cell trapping and perfusion methodology, with focusing and shield buffers, provides an innate "washing", minimizing reagent consumption, experiment time, and stress on the cell.

This experiment demonstrates the utility of this device for a common cellular assay. The device is also capable of supporting complex, multistep analyses. To demonstrate this latter capability, we have performed receptor-mediated cross-linking-dependent $[\text{Ca}^{2+}]_i$ measurements on human monocytic U937 cells.

Fc γ R-Mediated $[\text{Ca}^{2+}]_i$ Flux. A variety of leukocytes, including monocytes, macrophages, neutrophils, eosinophils, B-cells, and

(21) Rieder, C. L.; Cole, R. W. *Methods Cell Biol.* **1998**, *56*, 253–275.

(22) Takahashi, A.; Camacho, P.; Lechleiter, J. D.; Herman, B. *Physiol. Rev.* **1999**, *79*, 1089–1125.

(23) Mason, M. J.; Grinstein, S. *Biochem. J.* **1993**, *296*, 33–39.

(24) Dolmetsch, R. E.; Lewis, R. S. *J. Gen. Physiol.* **1994**, *103*, 365–388.

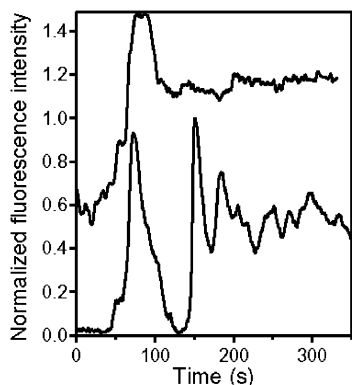


Figure 4. Ionomycin-mediated calcium flux measurements on two Jurkat T-cells. After perfusion with ionomycin, cells responded typically with ringing (lower trace) or with sustained $[Ca^{2+}]_i$ elevation (upper trace). Traces have been normalized and offset for comparison.

mast cells, express receptors ($Fc_\gamma R$) for the constant region of immunoglobulin G (IgG).^{25,26} $Fc_\gamma R$ -mediated signals are triggered by the “cross-linking” of multiple receptors in response to multiple ligand-binding events. Cross-linking initiates phosphorylation of intracellular kinases, which eventually results in initiation of the phosphoinositide cascade. Calcium is then released from internal stores and ultimately triggers degranulation, phagocytosis, cytokine release, or proinflammatory activation, depending on cell type.^{25, 26}

In vivo, cross-linking may occur in a single step, as an IgG-coated antigen interacts with multiple receptors. In vitro, $Fc_\gamma R$ cross-linking dynamics have been studied with multistep assays using the U937 human monocytic cell line.¹⁹ In these studies, changes in U937 $[Ca^{2+}]_i$ are observed as receptors are sequentially loaded with “primary antibody” (usually human IgG), followed by cross-linking with “secondary antibody” (usually anti-human IgG).^{27–29} In recent experiments, we have exploited this system for use as an immunity-based cell detector (R.J.W. and R.N.Z., submitted). These methodologies have typically required fluid change between steps, thus requiring relatively large volumes of antibody solutions (approximate microliters to milliliters).

In the present work, a solution of U937 cells (each $\sim 10 \mu m$ in diameter) was incubated with Fluo-4 calcium-indicating dye. Cells sometimes were differentiated with interferon- γ (IFN- γ) or dibutyryl cyclic AMP (dbcAMP) to promote varying $Fc_\gamma R$ expression prior to incubation. Individual cells were isolated on-chip and were then sequentially perfused with primary and secondary antibodies. For most experiments, primary antibody was perfused for 3 min, and cell fluorescence was observed during secondary antibody perfusion. High laser power or fast pumping frequency (which often results in cell vibration) occasionally caused unstimulated cells to respond. Thus, low excitation intensity ($2.5 \mu W$) and reduced pumping rates (5 Hz) were used. Control experiments of primary antibody (alone) and secondary antibody (alone) were performed to verify experimental validity (see Figure 5).

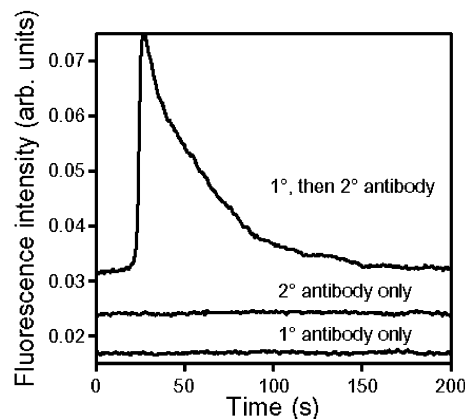


Figure 5. $Fc_\gamma R$ -mediated $[Ca^{2+}]_i$ measurements on three different U937 cells. One cell was perfused with primary antibody (human IgG) only (bottom), another cell with secondary antibody (goat anti-human IgG) only (middle), and a third cell with primary antibody (3 min) followed by secondary antibody (top). Antibody perfusion begins at $t = 0$ s (for top trace, only the secondary antibody perfusion step is shown). Traces have been offset vertically for comparison.

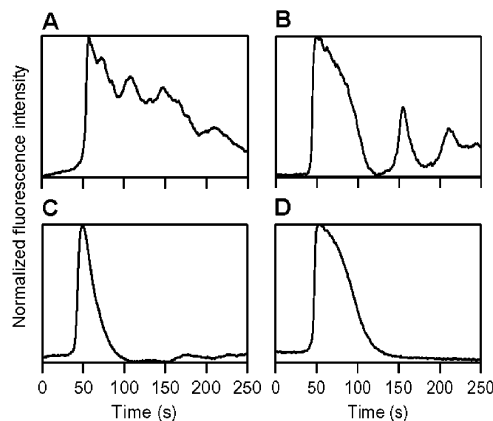


Figure 6. Representative $Fc_\gamma R$ -mediated $[Ca^{2+}]_i$ measurements on four U937 cells. All cells were perfused sequentially with primary antibody for 3 min, followed by secondary antibody, initiated at $t = 0$. These data are representative of commonly observed response types: ringing (A, B) and single spikes (C, D). Cells A and C were undifferentiated, cell B was differentiated with IFN- γ , and cell D was differentiated with dbcAMP. Traces have been normalized.

As has been previously reported,²⁸ $\sim 80\%$ ($n = 23/29$ cells) of cells responded to cross-linking with transient $[Ca^{2+}]_i$ increases; nonresponding cells' $[Ca^{2+}]_i$ did not change significantly over the observation time. Typical responses were 2–3 times the baseline (2.5 ± 0.8) in intensity. There was a 40 ± 20 s lag time between secondary antibody perfusion and calcium response; the average duration of response was 150 ± 80 s. Peak shapes varied widely from cell to cell as shown in Figure 6. This experiment demonstrates the capability of the device to perform multistep cell assays.

DISCUSSION

The microfluidic device described herein allows the capture of individual cells and the subsequent perfusion of reagents onto the selected cells. Thus, this system combines a highly miniaturized “perfusion chamber” with the unique advantages of single-cell analysis. We have demonstrated potential applications of this device by measuring intracellular calcium ion concentration in individual cells.

(25) Flesch, B. K.; Neppert, J. *J. Clin. Lab. Anal.* **2000**, *14*, 141–156.

(26) Ravetch, J. V.; Bolland, S. *Annu. Rev. Immunol.* **2001**, *19*, 275–290.

(27) Floto, R. A.; Mahaut-Smith, M.; Allen, J. M. *Biochem. Soc. Trans.* **1994**, *22*, 1225.

(28) Floto, R. A.; Mahaut-Smith, M.; Somasundaram, B.; Allen, J. M. *Cell Calcium* **1995**, *18*, 377–389.

(29) Davis, W.; Sage, S. O.; Allen, J. M. *Cell Calcium* **1994**, *16*, 29–36.

The results of the multistep receptor-mediated calcium flux experiment were particularly interesting. Despite significant differences in methodology (antibody loading time, experimental temperature, etc.), the magnitude, lag time, duration, and general peak shapes of our data agree remarkably well with the results of previous experiments.^{27–29} Thus, this system has demonstrated a functional microscale analogue of a multistep macroscale cell assay. Despite the general agreement with the literature noted above, a dependence of peak shape on differentiation^{27–29} with IFN- γ or dbcAMP was not observed (see Figure 6); this is perhaps attributable to methodological differences or differences in cell culture conditions.

The results presented demonstrate that this device can be used for a common cellular assay, the measurement of intracellular calcium. The small size (fits on a microscope coverslip) and versatility of the device should be useful for many variations²² of the methodology presented, including use of ratiometric indicating dyes, evaluation of biologically relevant ions other than calcium (such as potassium, magnesium, sodium, and hydrogen), and use of confocal microscopy.

A unique advantage of multilayer soft lithography fabrication is the ability to rapidly produce new device prototypes.¹² By making small changes in the design described herein, several

related devices have been developed for different methodologies, including simultaneous perfusion of multiple cells with different reagents and “cell dispensing” to collection chambers for culture. Our preliminary experiments (not shown) suggest that cell proliferation is not adversely affected by the PDMS microfluidic environment (3T3 cells have 15–24-h doubling times, which is consistent with the macroscale growth rate for these cells³⁰). Thus, the design described in this work is representative of a diverse family of devices that could be optimized for many different assays. Furthermore, each design could be scaled to accommodate hundreds of independent cell capture areas for use in high-throughput applications. This combination of adaptability and scalability could potentially revolutionize the way cellular assays are performed.

SUPPORTING INFORMATION AVAILABLE

Movie of a viability assay on a single cell. This material is available free of charge via the Internet at <http://pubs.acs.org>.

Note Added after ASAP Posting. The paper was posted 5/14/2003 before all corrections were made. The paper was reposted on 6/03/2003.

Received for review January 24, 2003. Accepted April 9, 2003.

AC0340758

(30) Todaro, G. J.; Green, H. J. *Cell Biol.* **1963**, *17*, 299–313.